

Classical and quantum magnetoresistance in a two-subband electron system

N. C. Mamani,¹ G. M. Gusev,¹ E. C. F. da Silva,¹ O. E. Raichev,^{1,2} A. A. Quivy,¹ and A. K. Bakarov^{1,3}

¹*Instituto de Física da Universidade de São Paulo, CP 66318 CEP 05315-970, São Paulo, SP, Brazil*

²*Institute of Semiconductor Physics, National Academy of Sciences of Ukraine, Prospekt Nauki 45, 03028 Kiev, Ukraine*

³*Institute of Semiconductor Physics, Novosibirsk 630090, Russia*

(Received 25 May 2009; published 7 August 2009)

We observe a large positive magnetoresistance in a bilayer electron system (double quantum well) as the latter is driven by the external gate from double to single layer configuration. Both classical and quantum contributions to magnetotransport are found to be important for explanation of this effect. We demonstrate that these contributions can be separated experimentally by studying the magnetic-field dependence of the resistance at different gate voltages. The experimental results are analyzed and described by using the theory of low-field magnetotransport in the systems with two occupied subbands.

DOI: [10.1103/PhysRevB.80.085304](https://doi.org/10.1103/PhysRevB.80.085304)

PACS number(s): 73.23.-b, 73.43.Qt, 73.21.Fg

I. INTRODUCTION

Magnetoresistance measurements are one of the most important and widely used tools for investigation of energy spectrum and scattering mechanisms of electrons in metals and semiconductors. For two-dimensional (2D) electron systems, studies of resistance in strong perpendicular magnetic fields have led to discoveries of the integer and fractional quantum Hall effect.¹ Currently, there is an interest to quantum transport phenomena occurring at relatively low magnetic fields in high-mobility 2D electron gas, in particular, the oscillations of resistivity and zero-resistance states in the presence of microwave irradiation.²⁻⁴ Together with the quantum magnetoresistance, the classical magnetoresistance remains the important subject of studies, since it is the main source of the data about carrier densities and mobilities.

The magnetotransport properties of low-dimensional electron gas are extensively studied in the strict 2D systems, where the transport is determined by electrons from a single (ground-state) size-quantized subband in a quantum well. A more sophisticated and less studied situation is realized in the quasi-2D systems, where two (or more) subbands are populated. The Fermi surface in this case comprises two (or more) different 2D branches (closed lines in the space of the 2D momentum), both of them contribute to the transport. For this reason, the magnetoresistance of the quasi-2D systems shows specific features which are not observed in the strict 2D systems. The Fermi surface consisting of two similar electronlike branches (circles) can be realized in a single quantum well at high enough electron density. More often, it is realized in double quantum wells (DQWs), see Ref. 5 and references therein, where the subband energy separation is typically on the order of several meV, and two-subband occupation is attainable even at low electron densities. The Fermi surface formed by hybridized electronlike and holelike branches is realized in the 2D systems obtained by using quantum wells with InAs/GaSb heterointerfaces⁶ and with gapless semiconductor layers.⁷ The two-subband systems described above are sensitive to the transverse electric fields induced by external gates,^{5,8} as well as to strong in-plane magnetic fields.^{9,10} Such fields considerably influence the magnetoresistance, since they change the subband popula-

tions and can lead to a substantial distortion of the Fermi surface, including a transition from double- to single-subband occupation.^{8,10}

The recent studies of magnetoresistance in high-mobility GaAs/AlGaAs DQWs have demonstrated^{11,12} the importance of quantum transport phenomena for the systems with two populated subbands in the region of low magnetic fields even at relatively high temperatures, when the Shubnikov-de Haas oscillations (SdHOs) of resistivity are suppressed. However, in spite of the progress in understanding the magnetotransport properties of these systems, some questions remain open. In particular, the problems of interplay of the classical and quantum contributions to the resistivity and of the influence of the variation in subband occupations on the magnetotransport have not been considered in detail. In this paper we undertake a systematic study of the low-field magnetotransport of high-mobility DQWs with high total sheet density of electrons ($n_s \simeq 10^{12} \text{ cm}^{-2}$), where both the subband populations and the scattering rates of electrons in the subbands are controlled by an external gate. By measuring both the magnetic-field and gate-voltage dependence of resistivity, we are able to distinguish experimentally between the classical and quantum contributions to magnetoresistance. We also report a large positive magnetoresistance induced and controlled by the gate voltage, and explain its physical origin. For analysis of the experimental data we apply the magnetotransport theory that takes into account both classical and quantum effects for two-subband systems. The experimental results are in good agreement with the results of theoretical calculations.

The paper is organized as follows. In Sec. II we list the basic expressions for description of low-field magnetotransport in DQWs. The experimental details, results of measurements, comparison of experiment and theory, and the discussion are presented in Sec. III. The concluding remarks are given in the last section.

II. MAGNETORESISTANCE OF 2D SYSTEMS WITH TWO POPULATED SUBBANDS

In weak enough magnetic fields, when the number of filled Landau levels is large, the resistivity of a 2D system

can be presented in analytic form, by expanding it with the accuracy up to the second order in Dingle factors

$$\rho_d = \rho_d^{(0)} + \rho_d^{(1)} + \rho_d^{(2)}, \quad (1)$$

where $\rho_d^{(0)}$ is the classical resistivity, $\rho_d^{(1)}$ is the first-order quantum contribution describing the SdHO, and $\rho_d^{(2)}$ is the second-order quantum contribution. It is necessary to take into account the last term, because it survives at high temperatures, in contrast to the SdHO term, which is strongly suppressed with increasing temperature. In application to the systems with two populated subbands (numbered below by the index $j=1,2$), the classical contribution to resistivity has been described theoretically in Ref. 13, while a systematic theory of the quantum contribution is given in Ref. 14. The summary of the equations presented below is based upon these references.

It is assumed that the temperature is low enough, so the electron gas is degenerate, and the main scattering mechanism for electrons is the elastic scattering by impurities or other inhomogeneities. Thus, all the contributions in Eq. (1) can be expressed through the elastic quantum relaxation rates $\nu_{jj'}$ and transport scattering rates $\nu_{jj'}^r$, at the Fermi surface. The latter represents itself two concentric circles, because the system is isotropic in the 2D plane. The classical resistivity is conveniently presented as

$$\rho_d^{(0)} = \frac{m}{e^2 n_s} \frac{\omega_c^2 \nu_s + \nu_0 \nu_r^2}{\omega_c^2 + \nu_r^2}, \quad (2)$$

where $n_s = n_1 + n_2$ is the total electron density, n_1 and n_2 are the electron densities in the subbands, and ω_c is the cyclotron frequency. This contribution increases with the magnetic field, starting from the zero-field value $\rho_0^{(0)} = m\nu_0/e^2 n_s$, and saturates at $\omega_c \gg \nu_r$ with the value $\rho_{sat}^{(0)} = m\nu_s/e^2 n_s$. The characteristic rates ν_s , ν_r , and ν_0 are given by

$$\nu_s = (n_1/n_s)\nu_{11}^r + (n_2/n_s)\nu_{22}^r + \nu_{12}^r, \quad (3)$$

$$\nu_r = (n_2/n_s)\nu_{11}^r + (n_1/n_s)\nu_{22}^r + 2\nu_{12} - \nu_{12}^r, \quad (4)$$

$$\nu_0 = D/\nu_r, \quad D = (\nu_{11}^r + \nu_{12})(\nu_{22}^r + \nu_{12}) - (\nu_{12} - \nu_{12}^r)^2 n_s^2 / 4n_1 n_2. \quad (5)$$

The increase in $\rho_d^{(0)}$ with the magnetic field is stronger if the difference between ν_{11}^r and ν_{22}^r is larger. The mechanism of such positive magnetoresistance is similar to that for two groups of carriers with different mobilities. However, owing to the intersubband coupling via scattering, the term $\rho_d^{(0)}$ is not reduced simply to the contribution given by two independent groups of carriers from the first and second subbands.

The first-order quantum contribution is

$$\rho_d^{(1)} = -\frac{T}{e^2 n_s} \sum_{j=1,2} \left[\frac{2n_{sj}}{n_s} \nu_{jj}^r + \nu_{12}^r \right] \exp(-\alpha_j) \cos \frac{2\pi(\varepsilon_F - \varepsilon_j)}{\hbar\omega_c}, \quad (6)$$

where $\alpha_j = \pi\nu_j/\omega_c$ with $\nu_j = \nu_{jj} + \nu_{12}$ are the Dingle exponents, ε_j are the subband energies, and $T = X/\sinh X$ with $X = 2\pi^2 T/\hbar\omega_c$ is the thermal suppression factor. Finally,

$$\rho_d^{(2)} = \frac{2m}{e^2 n_s} \left[\frac{n_1}{n_s} \nu_{11}^r e^{-2\alpha_1} + \frac{n_2}{n_s} \nu_{22}^r e^{-2\alpha_2} + \nu_{12}^r e^{-\alpha_1 - \alpha_2} \cos \frac{2\pi\Delta_{12}}{\hbar\omega_c} \right]. \quad (7)$$

This term describes both the positive magnetoresistance and the magnetointersubband (MIS) oscillations,¹¹ whose maxima correspond to integer ratios of the subband splitting energy $\Delta_{12} = \varepsilon_2 - \varepsilon_1$ to the cyclotron energy $\hbar\omega_c$.

The rates $\nu_{jj'}$, which stand in the Dingle factors, and transport scattering rates $\nu_{jj'}^r$ are determined by the expressions

$$\left. \begin{array}{l} \nu_{jj'} \\ \nu_{jj'}^r \end{array} \right\} = \frac{m}{\hbar^3} \int_0^{2\pi} \frac{d\theta}{2\pi} w_{jj'}[\sqrt{(k_j^2 + k_{j'}^2)} F_{jj'}(\theta)] \times \left\{ \begin{array}{l} 1 \\ F_{jj'}(\theta) \end{array} \right., \quad (8)$$

where $w_{jj'}(q)$ are the Fourier transforms of the correlators of the scattering potential, $F_{jj'}(\theta) = 1 - 2k_j k_{j'} \cos \theta / (k_j^2 + k_{j'}^2)$, θ is the scattering angle, and $k_j = \sqrt{2\pi n_j}$ is the Fermi wave number for the subband j .

III. RESULTS AND DISCUSSION

The samples under investigation are symmetric GaAs/GaAlAs DQWs with 14-nm-wide wells and different barrier thicknesses $d_b = 1.4, 2,$ and 3 nm. The densities in the wells are variable by a gold top gate. The voltage of the gate, V_g , changes the density of the well closest to the sample surface, with carrier density in the other well being almost constant. The system is balanced (has equal densities in the wells) at $V_g = 0$. The samples are processed in the Hall bar geometry with $L_x/L_y = 2.5$, where L_x is the distance between the voltage probes and L_y is the bar width. By investigating the magnetic-field and gate-voltage dependence of resistivity, we obtain similar results for different samples in the interval of temperatures T from 1.4 to 20 K. The results described below are obtained at $T = 4.2$ K for the sample with $d_b = 1.4$ nm, 2D electron mobility of 8×10^5 cm²/V s at $V_g = 0$ and $B = 0$, and total sheet density $n_s = 0.94 \times 10^{12}$ cm⁻² at $V_g = 0$. The subband separation $\Delta_{12} = 3.3$ meV for the case of balanced DQWs is found from the MIS oscillation periodicity at low B .

The measured magnetic-field dependence of the dissipative resistance $R = R_{xx}$ at different (negative) gate voltages is shown in Fig. 1. In the absence of the bias ($V_g = 0$) we see the MIS oscillations at low magnetic fields, while at $B > 1$ T the magnetoresistance is dominated by the SdHO. As $|V_g|$ increases, one can distinguish several regimes of magnetotransport. First, relatively small voltages up to 0.55 V lead to suppression of the MIS oscillations and slow increase in the resistivity with the magnetic field. Next, approximately at $|V_g| = 0.7$ V, the magnetoresistance starts to increase faster in the low-field region. This rapid increase is changed to a slower one at higher magnetic fields. The curves plotted at $|V_g| = 0.8$ and 0.9 V are representative for this regime. Finally, starting from 1 V, we see a fast suppression of magnetoresistance by the applied voltage, which is associated with depletion of the upper subband 2 and with transition to a

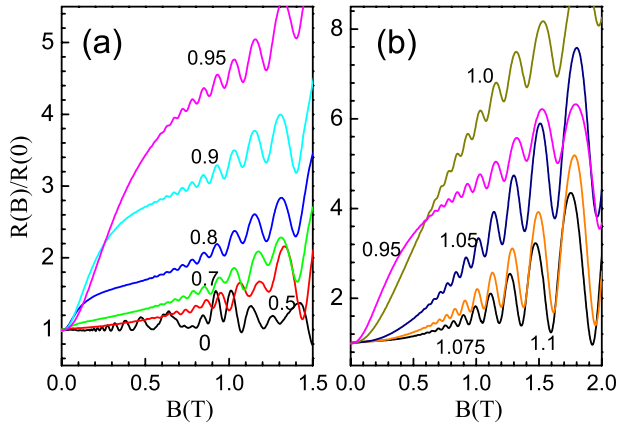


FIG. 1. (Color online) Resistance of the DQWs as a function of magnetic field at the temperature $T=4.2$ K and different gate voltages. The values of $-V_g$ in volts are indicated for each plot.

single-subband transport. According to our estimates, the depletion occurs approximately at $V_g = -1.1$ V. We denote the corresponding depletion voltage as V_{g0} .

The gate-voltage dependence of resistivity at several magnetic fields is shown in Fig. 2. Here we can see a peak in the resistivity even at $B=0$. With increasing B , the peak steadily increases, and its maximum moves closer to the point of depletion of the upper subband. Further increase in $|V_g|$ after passing this depletion point again leads to the increasing resistivity, because the applied voltage starts to deplete the lower subband when the upper one is already depleted. The relative heights of the peaks are indicated in the inset, where R_{\max} is the resistance in the maximum and $R_0 \approx 20 \Omega$ is the zero-gate resistance at $B=0$. The dependence of R_{\max} on the field is approximately linear.

Our explanation of the observed features is based on the formalism presented in Sec. II. At weak magnetic fields, when the SdHO contribution $\rho_d^{(1)}$ is thermally suppressed, the resistance is determined by the classical component $\rho_d^{(0)}$ and

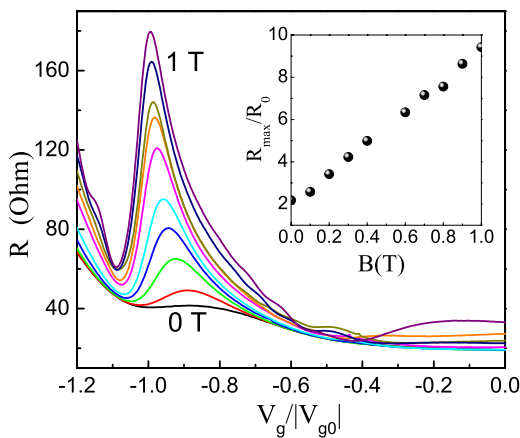


FIG. 2. (Color online) Resistance of the DQWs as a function of gate voltage at the temperature $T=4.2$ K and different magnetic fields. The ten plots with monotonically enhanced peaks correspond to B from 0 to 0.4 T and from 0.6 to 1 T with the interval of 0.1 T. The inset shows the relative increase in the resistance in the maximum.

quantum component $\rho_d^{(2)}$. The classical magnetoresistance is large when the transport rates ν_{11}^r and ν_{22}^r [see Eq. (8)] strongly differ from each other; the mechanism of this effect is the same as in the case of two groups of carriers with different mobilities. Since our DQWs are symmetrically doped, which means $w_{11}(q) = w_{22}(q)$, the difference in ν_{11}^r and ν_{22}^r can be obtained when the difference in Fermi wave numbers k_1 and k_2 is considerable and the scattering potentials are long range correlated, i.e., the dependence of w_{jj} on the scattering angle is strong. For electrons in the lower subband, whose density is large, the case of long-range scattering potentials means small-angle scattering of low probability ($\theta \ll 1$). For electrons in the second subband, whose density (and, accordingly, the Fermi wave number k_2) is reduced by the gate, the scattering probability increases because the region of scattering angles θ becomes broader. The above consideration shows that the classical magnetoresistance is expected to increase as the upper subband is depleted. However, when the density of the electrons in this subband becomes very low and they cannot efficiently contribute to the transport, the magnetoresistance decreases again. Therefore, the classical component $\rho_d^{(0)}$ should have a maximum as a function of the gate voltage, and we attribute the observed maximum in Fig. 2 mostly to the classical contribution. Indeed, we have the case of long-range scattering potentials, because for all our samples the quantum relaxation rate, estimated from the amplitudes of the MIS oscillations,¹¹ is more than one order of magnitude greater than the transport scattering rate found from zero-field mobility.

The classical magnetoresistance, however, remains weak for moderate gate voltages, when the difference between k_1 and k_2 is small. Next, the classical magnetoresistance saturates with the increasing magnetic field; see Eq. (2) and Ref. 15. In these regions of parameters the quantum magnetoresistance becomes important. The quantum magnetoresistance is not strong at weak magnetic fields because it is proportional to the small Dingle factors. At higher fields it increases and does not saturate, so we explain the absence of saturation of the peak height in Fig. 2 by the presence of the quantum component of magnetoresistance.

When the voltage is applied to the gates, its first effect is the suppression of the MIS oscillations, because the intersubband scattering is reduced as the system is driven out of the balance and the wave functions for the subbands 1 and 2 become localized in the different wells.¹¹ The difference in the subband occupations is not yet large at such voltages, and the quantum contribution dominates over the classical one, leading to a slow increase in magnetoresistance. At higher negative voltages we enter the regime where the resistance, as a function of B , increases faster in the low-field region, owing to the classical contribution. Since the latter is saturated at certain values of the magnetic field, the slope of the B dependence of the resistance is changed (see the plots for $|V_g| = 0.8$ and 0.9 V in Fig. 1). By increasing $|V_g|$ further on, we increase the resistance until the region when the density of electrons in the upper subband becomes very low. Then the resistance rapidly drops down with increasing $|V_g|$.

For quantitative description of the results, we assume that the lower subband population n_1 stays independent of the

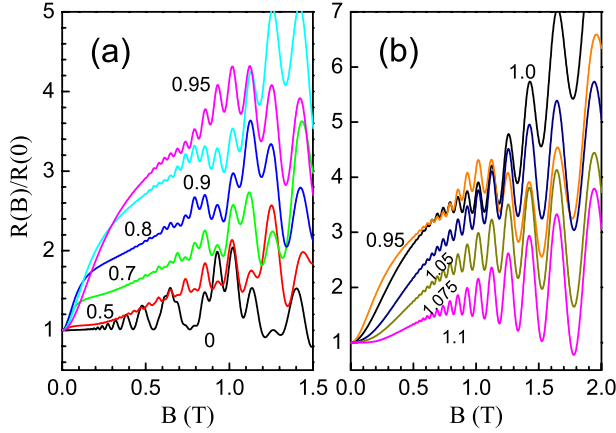


FIG. 3. (Color online) Calculated normalized resistance of the DQWs as a function of magnetic field at $T=4.2$ K, corresponding to the measurements shown in Fig. 1. The values of $-V_g$ in volts are indicated.

gate voltage. This assumption approximately correlates with our experimental data. The depletion of the upper subband is determined by the general relation $n_2 = n_1 - \rho_{2D} \Delta_{12}$, where $\rho_{2D} = m / \pi \hbar^2$ is the 2D density of states (in the spin-degenerate case that we consider). The subband separation is given by the expression $\Delta_{12} = \sqrt{\Delta_{SAS}^2 + \Delta^2}$, where Δ_{SAS} is the subband separation in balanced DQWs. The parameter Δ , which is proportional to the difference of the electron densities in the left and right wells, is assumed to scale linearly with the applied gate voltage, according to electrostatic properties of DQWs. To describe the gate dependence of the scattering rates [see Eq. (8)], we model the scattering potentials by the Gaussian correlation function $w_{jj'}(q) = w_{jj'} \exp(-l_c^2 q^2 / 2)$, where l_c is the correlation length. The amplitudes $w_{jj'}$ are estimated for the case when the interlayer correlations of the potential are neglected, which gives for the symmetric DQWs (Ref. 14) $w_{11} = w_{22} = w_0(1 + \delta^2)/2$ and $w_{12} = w_0(1 - \delta^2)/2$, where $\delta = \Delta / \Delta_{SAS}$. The two parameters of the model, w_0 and l_c , are determined from the measured quantities: zero-field resistance and amplitude of the quantum contribution (MIS oscillations) in balanced DQWs ($V_g = 0$) at low magnetic fields. The correlation length found from these data is 14.5 nm, and the ratio of the averaged quantum relaxation rate to the averaged transport scattering rate is 11.7 for balanced DQWs.

Figure 3 shows the magnetic-field dependence of the resistance, calculated as described above. The calculations are carried out for the same gate voltages as in Fig. 1. The plots demonstrate a good qualitative agreement with the results of measurements, indicating transitions between different transport regimes as the gate voltage changes. We do not expect a complete quantitative agreement, since we have used model assumptions about the scattering potential and a simplified description of the depletion of electrons by the gate. A detailed comparison of experiment and theory is presented in Fig. 4 for the most interesting regime, when the classical contribution to resistivity saturates with increasing magnetic field, and the lowering slope of the B dependence of the resistance indicates a transition from the classical to the quantum magnetoresistance. We may see, that the theory is

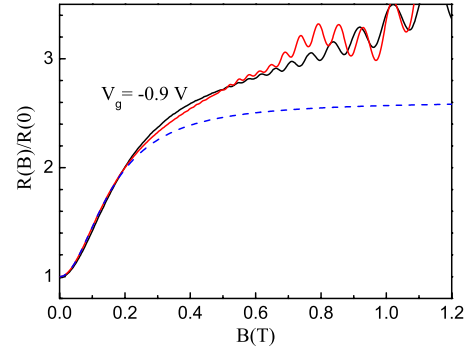


FIG. 4. (Color online) Comparison of measured and calculated magnetoresistance of the DQWs for $V_g = -0.9$ V at $T = 4.2$ K. The dashed line is the calculated classical contributions showing saturation with increasing field.

in a quantitative agreement with the experiment as concerns the magnitudes of the resistivity slopes in the classical and quantum magnetoresistance regions. Thus, we indeed can separate the classical and quantum magnetoresistance of DQWs by using the experimental data. These data can be applied in order to find the dependence of the quantum relaxation rate and transport scattering rate for the upper subband 2 on the density n_2 , which is varied by the gate voltage. Whereas we have found that this dependence is reasonably described by the simple Gaussian-correlation model of the scattering potential, a more detailed characterization of this potential is possible from magnetotransport measurements.

In Fig. 5 we show the calculated gate-voltage dependence of the resistivity at different magnetic fields. The plots clearly reproduce the most important features observed in the experiment, the continuous increase in the peaks and the shift of the peak positions to more negative voltages as the magnetic field increases. One can also see the importance of the quantum contribution to the resistivity in the peak region. On the other hand, the theoretical peaks are broader and

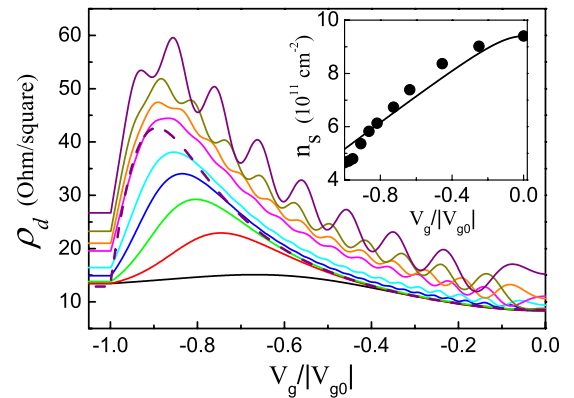


FIG. 5. (Color online) Calculated resistivity of the DQWs as a function of gate voltage at the temperature $T = 4.2$ K and different magnetic fields. The solid lines correspond to $B = 0, 0.1, 0.2, 0.3, 0.4, 0.6, 0.7, 0.8,$ and 1 T. The dashed line shows the classical component of the resistivity at 1 T. The inset demonstrates how the total sheet density decreases as a function of the gate voltage according to the Hall measurements (points) and theoretical model (line).

lower (the theoretical ratio R_{\max}/R_0 is equal to 6.5 at $B = 1$ T, while the corresponding experimental ratio is 9.3). The main difference between the theory and the experiment is the presence of the SdHO as a function of voltage in the peak region, while the oscillations in the corresponding experimental plots are less pronounced and completely disappear in the peak region. A possible explanation of this behavior is that application of the gate voltage not only changes the electron density but also increases scattering by modifying the density distribution across the double well. The suppression of screening owing to lowering of the electron density also leads to increased scattering. Most probably, the gate voltage also enhances long-range inhomogeneities of the system, and the SdHOs are significantly reduced because of inhomogeneous broadening effect. The MIS oscillations are also suppressed by the gate voltage faster than predicted by the theory. To take into account all these effects, a detailed consideration of the scattering mechanisms and electrostatic potentials in the DQWs is necessary, which is beyond the scope of the present paper. On the other hand, the nonoscillating part of the quantum resistivity $\rho_d^{(2)}$ is not suppressed by the inhomogeneous broadening, and our analysis shows that it essentially contributes to the effect of large magnetoresistance we observe.

IV. SUMMARY AND CONCLUSIONS

By varying the voltage at the gate to the double quantum-well system with high electron density and reasonably high mobility, we have found a large increase in the resistivity of electron gas in the presence of perpendicular magnetic field B . Even in the field as weak as 1 T, the peak resistance is about one order of magnitude greater than the zero-field resistance at zero gate voltage. This magnetoresistance is much larger than that previously observed for similar systems (see Refs. 5 and 8).

We explain the observed effect of the gate by a strong enhancement of the probability of elastic scattering for electrons in the upper subband when this subband is close to the

point of depletion. The proposed mechanism of this enhancement essentially requires that the electrons are scattered mostly by the long-range disorder potential. This condition is satisfied in our samples. Next, our samples have high electron densities, which is also preferable for observation of the effect.

The gate-induced magnetoresistance enhancement is attributed to the increase in the classical contribution to resistivity. In addition, in our samples we observe a considerable influence of the quantum contribution, which is a manifestation of the Landau quantization in magnetotransport. Apart from the Shubnikov-de Haas oscillations and magnetointer-subband oscillations specific for the two-subband systems, the quantum contribution contains a nonoscillating part describing positive magnetoresistance. In the case of single-subband occupation, such positive magnetoresistance is also seen experimentally,¹⁶ and its systematic theoretical description is given in Ref. 17. This part adds to the classical contribution and leads to a further enhancement of the observed resistance in magnetic fields. The nonoscillating quantum contribution is almost insensitive to the gate voltage. However, in contrast to the classical contribution that saturates as a function of the magnetic field, the quantum contribution continuously increases with the field. This property enables us to separate the two contributions by investigating the magnetic-field dependence of the resistance at different gate voltages.

Finally, we have demonstrated that the observed magnetic-field and gate-voltage dependence of the resistance of DQWs are in full qualitative agreement with the theory of low-field magnetotransport in two-subband systems, which describes the effects of Landau quantization with the accuracy up to the second order in the Dingle factors. The reliability of this theoretical approach is, therefore, confirmed in application to DQWs.

ACKNOWLEDGMENTS

This work was supported by FAPESP and CNPq (Brazilian agencies).

¹*Perspectives in Quantum Hall Effects: Novel Quantum Liquids in Low-Dimensional Semiconductor Structures*, edited by S. Das Sarma and A. Pinczuk (Wiley-Interscience, New York, 1996).

²M. A. Zudov, R. R. Du, J. A. Simmons, and J. L. Reno, *Phys. Rev. B* **64**, 201311(R) (2001).

³R. G. Mani, J. H. Smet, K. von Klitzing, V. Narayanamurti, W. B. Johnson, and V. Umansky, *Nature (London)* **420**, 646 (2002).

⁴M. A. Zudov, R. R. Du, L. N. Pfeiffer, and K. W. West, *Phys. Rev. Lett.* **90**, 046807 (2003).

⁵R. Fletcher, M. Tsousidou, T. Smith, P. T. Coleridge, Z. R. Wasilewski, and Y. Feng, *Phys. Rev. B* **71**, 155310 (2005).

⁶M. J. Yang, C. H. Yang, B. R. Bennett, and B. V. Shanabrook, *Phys. Rev. Lett.* **78**, 4613 (1997).

⁷Z. D. Kvon, E. B. Olshanetsky, D. A. Kozlov, N. N. Mikhailov, and S. A. Dvoretzky, *JETP Lett.* **87**, 502 (2008).

⁸Y. Katayama, D. C. Tsui, H. C. Manoharan, S. Parihar, and M. Shayegan, *Phys. Rev. B* **52**, 14817 (1995).

⁹G. S. Boebinger, A. Passner, L. N. Pfeiffer, and K. W. West, *Phys. Rev. B* **43**, 12673 (1991).

¹⁰J. A. Simmons, S. K. Lyo, N. E. Harff, and J. F. Klem, *Phys. Rev. Lett.* **73**, 2256 (1994).

¹¹N. C. Mamani, G. M. Gusev, T. E. Lamas, A. K. Bakarov, and O. E. Raichev, *Phys. Rev. B* **77**, 205327 (2008).

¹²S. Wiedmann, G. M. Gusev, O. E. Raichev, T. E. Lamas, A. K. Bakarov, and J. C. Portal, *Phys. Rev. B* **78**, 121301(R) (2008).

¹³E. Zaremba, *Phys. Rev. B* **45**, 14143 (1992).

¹⁴O. E. Raichev, *Phys. Rev. B* **78**, 125304 (2008).

¹⁵If intersubband scattering is neglected, the saturated magnetoresistance is given by a simple formula $\rho_{\text{sat}}^{(0)}/\rho_{B=0}^{(0)} = 1 + (n_1 n_2 / n_s^2) (v_{11}^r - v_{22}^r)^2 / v_{11}^r v_{22}^r$.

¹⁶See, for example, V. Renard, Z. D. Kvon, G. M. Gusev, and J. C. Portal, *Phys. Rev. B* **70**, 033303 (2004).

¹⁷M. G. Vavilov and I. L. Aleiner, *Phys. Rev. B* **69**, 035303 (2004).